

RepetitionCurse: Measuring and Understanding Router Imbalance in Mixture-of-Experts LLMs under DoS Stress

Ruixuan Huang¹ Qingyue Wang¹ Hantao Huang² Yudong Gao¹ Dong Chen¹ Shuai Wang¹ Wei Wang¹

Abstract

Mixture-of-Experts architectures have become the standard for scaling large language models due to their superior parameter efficiency. To accommodate the growing number of experts in practice, modern inference systems commonly adopt expert parallelism to distribute experts across devices. However, the absence of explicit load balancing constraints during inference allows adversarial inputs to trigger severe routing concentration. We demonstrate that out-of-distribution prompts can manipulate the routing strategy such that all tokens are consistently routed to the same set of top- k experts, which creates computational bottlenecks on certain devices while forcing others to idle. This converts an efficiency mechanism into a denial-of-service attack vector, leading to violations of service-level agreements for time to first token. We propose RepetitionCurse, a low-cost black-box strategy to exploit this vulnerability. By identifying a universal flaw in MoE router behavior, RepetitionCurse constructs adversarial prompts using simple repetitive token patterns in a model-agnostic manner. On widely deployed MoE models like Mixtral-8x7B, our method increases end-to-end inference latency by 3.063 \times , degrading service availability significantly.

1. Introduction

The capabilities of large language models (LLMs) continue to advance rapidly (Cai et al., 2025; Li et al., 2025a), but deploying dense models at scale incurs prohibitive computational and memory costs. To address this challenge, the Mixture-of-Experts (MoE) architecture (Shazeer et al., 2017) has emerged as a practical solution by sparsely activating only a subset of experts during inference, enabling substantially larger models to be deployed under fixed resource budgets.

¹HKUST, Hong Kong ²NTU, Singapore. Correspondence to: Qingyue Wang <qingyue.wang@ust.hk>.

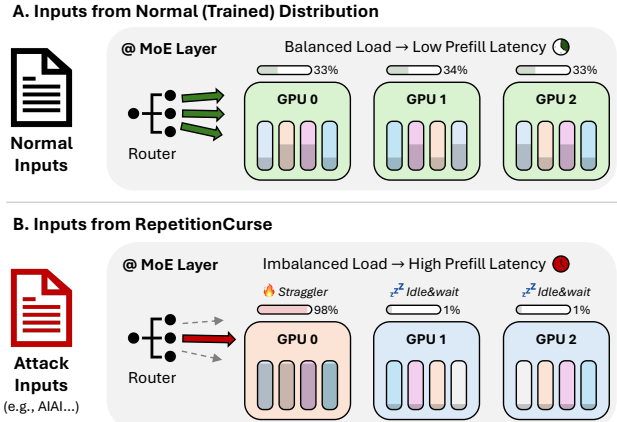


Figure 1. RepetitionCurse attack overview. Under attack inputs, all tokens are routed to the same top- k experts, causing a single GPU to become a straggler while other GPUs have to idle and wait.

The MoE architecture introduces a fundamentally different model structure compared to dense models. Instead of a single monolithic feed-forward network (FFN) per layer, MoE layers contain multiple independent expert networks, with a router dynamically selecting a small subset of experts for each token. This structural independence makes conventional tensor parallelism (TP), which partitions individual operators across devices (Shoeybi et al., 2019) inefficient for MoE inference. Instead, MoE models are naturally deployed using expert parallelism (EP), where distinct experts are entirely hosted on different physical devices (Du et al., 2022; Fedus et al., 2021), which minimizes inter-GPU communication and maximizes memory efficiency.

However, this design also introduces a fragile dependency on the token-to-expert routing distribution (Mu & Lin, 2025), creating a significant attack surface for Denial-of-Service (DoS) vulnerabilities, as illustrated in Figure 1. During training, MoE models utilize expert and device balance losses or bias (DeepSeek-AI et al., 2024a;b) to enforce load balancing, expecting all experts to be trained evenly. However, these explicit constraints are typically absent during inference. Under natural language inputs, the router's generalization ability results in a relatively uniform distribution of tokens across experts. In this paper, we demonstrate that

this assumption is easily broken. We reveal that attackers can craft adversarial inputs, specifically utilizing repetitive token patterns that override the router’s training distribution. These inputs induce extreme routing imbalance, where the workload is targeted at a few bottleneck experts and their hosting GPUs. With EP, this forces all other GPUs to idle while waiting for the straggler device to complete its computation. This behavior constitutes an algorithmic DoS attack: by exploiting the architectural logic rather than flooding network bandwidth, **an attacker can consume system resources multiplicatively and degrade service latency for all users within its batch.**

We introduce RepetitionCurse, a simple yet highly effective method to generate these DoS prompts that can cause router imbalance. Unlike adversarial attacks that require gradient access or searching (Zou et al., 2023; Hayes et al., 2024), RepetitionCurse operates effectively in black-box settings. Our investigation of 139 MoE configurations with the most downloads on Huggingface reveals that **nearly all current models are susceptible to this vulnerability**. Our experiments show that on Mixtral-8x7B API, RepetitionCurse amplifies prefilling latency by $3.063 \times$ (Section 4.2), turning the system’s parallelism against itself. This creates a dilemma for hardware providers during deployment: **they are discouraged from using large-scale EP, as the system becomes increasingly vulnerable to these attacks as the degree of parallelism grows**. As commercial inference services increasingly adopt highly sparse MoE models (e.g., DeepSeek-V3), this attack vector warrants urgent attention.

Beyond service degradation, we uncover that this vulnerability poses a privacy risk. Since the latency spike is intrinsic to the physical deployment of experts, we demonstrate that an attacker can observe response times to infer hidden backend information, such as whether the target is an MoE model. Our contributions are summarized as follows:

- We identify a widespread DoS vulnerability in EP-based MoE serving systems caused by routing imbalance.
- We propose RepetitionCurse, a black-box attack method that uses repetitive tokens to induce router imbalance.
- We demonstrate that routing latency serves as a side-channel for inferring backend model architecture.

Mitigation: Since RepetitionCurse is a newly proposed attack vector, we propose defense strategies in Section 5.3 to ensure ethical compliance.

2. Backgrounds

2.1. Inference of Transformer-based LLMs

The Transformer architecture serves as the fundamental backbone for current LLMs (Vaswani et al., 2017; Sun et al.,

2025). The body of an LLM is constructed by stacking multiple Transformer blocks. Each block typically comprises a self-attention layer and a feed-forward network (FFN) layer. An FFN layer generally consists of two MLP layers. MoE models are replacing the dense FFN layers with MoE layers.

The inference of Transformer-based autoregressive LLMs proceeds in two phases:

- **Prefill:** The model processes the entire input sequence in parallel, computing the attention keys and values for all input tokens and populating the initial KV cache. The prefill phase is *compute-bound*, with its heavy computational load to process the full input sequence.
- **Decoding:** The model generates output tokens sequentially in an autoregressive manner. The decoding phase is *memory-bound* due to the high memory bandwidth overhead incurred by frequent access to the KV cache.

Modern inference engines, such as vLLM (Kwon et al., 2023) and SGLang (Zheng et al., 2024), employ prefill-decoding separation strategies to allocate these phases to distinct hardware resources for improved performance. As a result, the latency of the prefill phase directly impacts the time to first token (TTFT), a key metric for interactive LLM serving (Agrawal et al., 2024), potentially violating latency-sensitive service-level agreements (Gong et al., 2025).

2.2. Mixture-of-Expert Models with Expert Parallelism

Distinct from dense models, an MoE layer comprises multiple weight-independent experts. For each input token, only a small subset of these experts is activated. Formally, considering a model containing E experts per layer and input hidden state h , one MoE layer first determines the participation of experts via the logits provided by the router:

$$G(h) = \text{Softmax}(h \cdot W_{\text{router}}) \in \mathbb{R}^E \quad (1)$$

where W_{router} is the weight of the router. Then, based on Top- k routing strategy, the top- k experts (denoted as \mathcal{E}) with the highest router logits are selected to process the token:

$$y = \sum_{i \in \mathcal{E}} G(h)_i \cdot E_i(h) \quad (2)$$

Under expert parallelism (EP), the complete weights of one or more experts are hosted on a single GPU. Modern inference engines employ fused kernels, such as grouped GEMM (vLLM Contributors, 2025), to jointly execute the computation for all experts residing on the same GPU. The execution time of these fused kernels is determined by the number of assigned tokens, rather than the load of individual experts. Consequently, load balance in EP is measured at the GPU level instead of the expert level.

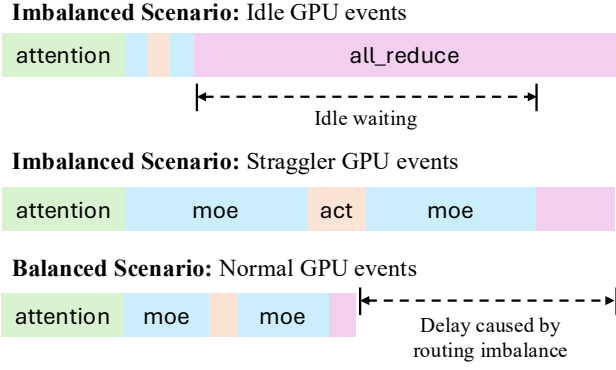


Figure 2. GPU event timeline under both balanced and imbalanced routing for a single MoE layer computation. Unrelated events such as normalization are omitted.

The EP execution is highly sensitive to routing distribution. When router imbalance occurs, GPUs with lighter loads must idle and wait for the straggler GPU to complete before initiating the inter-GPU all-reduce synchronization. Figure 2 illustrates the GPU event timeline under both balanced and imbalanced routing for a single MoE layer computation. According to Amdahl’s Law (Amdahl, 1967), since the MoE computation constitutes the majority of the inference runtime, any elongation of this critical path significantly exacerbates end-to-end latency.

3. Attack Methodologies

3.1. Threat Model

Asset Owner: In this paper, we define the asset owner as the service provider who deploys MoE-based LLMs on a multi-GPU cluster with EP to serve users via public APIs.

Attack Objective: The attacker aims to launch an algorithmic DoS attack to exhaust resources of the target LLM service. By submitting adversarial requests, the attacker seeks to inflate the queuing time for legitimate user requests, and to degrade the service’s responsiveness and reliability. By utilizing prompt strategies that induce maximal latency, the attacker can achieve significant service degradation with minimal query cost.

Attacker Capabilities: The attacker is permitted to send input queries to the API but possesses no knowledge of the backend architecture, including whether an MoE model is being utilized. The attacker disregards the quality of the model’s output, as the attack vectors target the computational costs during the prefill phase of inference.

3.2. Adversarial Prompt Formulation

The adversarial prompt needs to let MoE models route its tokens to the same combination of Top- k experts as much as

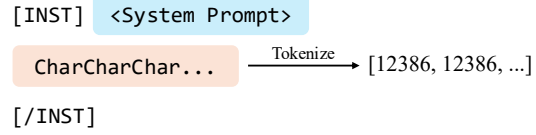


Figure 3. Illustration of RepetitionCurse prompt.

possible to create a bottleneck. In this paper, we introduce a very simple method to construct the near optimal adversarial prompts called RepetitionCurse, where **all tokens are set to be the same** except for the instruction template and system prompt (see Figure 3). RepetitionCurse is simple and practically optimal, doesn’t need search or optimization and it can generally span different contexts and system prompts (Section 5.1), thus having the potential for black-box attacks.

3.3. Measurement of Attack Performance

We first explore the capabilities of RepetitionCurse through a locally deployed open-source LLM API by vLLM. To systematically evaluate the prevalence of the router imbalance vulnerability, we establish a formal framework describing the MoE deployment. Consider an MoE model with a vocabulary \mathcal{V} . Let $\mathcal{E}_l = \{e_{l,1}, \dots, e_{l,E}\}$ denote the set of experts at the l -th layer. The model is deployed across a set of physical devices, denoted as $\mathcal{D} = \{d_1, \dots, d_M\}$. Based on EP strategy, we define a mapping function $\mathcal{M}_l : \mathcal{D} \rightarrow 2^{\mathcal{E}_l}$, which assigns a subset of experts to a specific device d , representing a deployment configuration.

Theoretical Upper Bound Analysis. We derive the theoretical limit of load concentration caused by RepetitionCurse under a specific deployment configuration. Assuming each GPU hosts $E_d = |\mathcal{M}_l(d)|$ experts and the routing strategy is top- k , the theoretical maximum imbalance (TMI), defined as the ratio of the worst-case single-device load to the ideal balanced load, is governed by k and E_d :

$$\text{TMI} = \frac{\min(k, E_d)}{k/|\mathcal{D}|} = |\mathcal{D}| \cdot \frac{\min(k, E_d)}{k} \quad (3)$$

Equation (3) reveals two distinct regimes. For sparser models like DeepSeek-V3 ($k \leq E_d$), the attacker can achieve the perfect bottleneck when scaling the EP size. For models like Mixtral-8x7B under high-degree parallelism (e.g., $|\mathcal{D}| = 8 \Rightarrow E_d = 1 < k = 2$), the selected experts are physically forced to span multiple devices. Hence, the bottleneck is capped at $|\mathcal{D}|/k$.

Real-world Constraints. TMI characterizes a static worst-case attack scenario under experts concentration. In practice, inference engines assign experts to GPUs in a fixed numerical order by default, but dynamic mechanisms like Expert Parallelism Load Balancer (EPLB) (DeepSeek-AI, 2025) periodically reconfigure expert-GPU mappings based on

observed workloads. While such reallocation can mitigate routing imbalance, it is performed at coarse time scales (e.g., minutes) and incurs non-negligible overhead; within each relocation window, the expert layout remains static.

Coverage. While TMI defines the potential upper limit, we introduce a coverage metric to quantify the empirical vulnerability of any MoE model across its entire vocabulary \mathcal{V} under a snapshot of the deployment landscape. For a RepetitionCurse prompt P_t constructed using a specific token $t \in \mathcal{V}$, let $\rho_e(P_t)$ represent the percentage of tokens routed to expert e . We calculate the computational load $L_{l,d}(P_t)$ for device d at layer l , and then the total bottleneck $B(P_t)$ for the model across all layers:

$$\left\{ \begin{array}{l} L_{l,d}(P_t) = \frac{1}{|\mathcal{M}_l(d)|} \sum_{e \in \mathcal{M}_l(d)} \rho_e(P_t) \\ B(P_t) = \frac{1}{L} \sum_{l=1}^L \max_{d \in \mathcal{D}} L_{l,d}(P_t) \end{array} \right. \quad (4)$$

To determine the proportion of the vocabulary that can be exploited, we iterate through every token $t \in \mathcal{V}$, construct its corresponding RepetitionCurse prompt, and compute the average bottleneck $\mathcal{B} = \sum_{t \in \mathcal{V}} B(P_t) / |\mathcal{V}|$, which represents the **proportion of the optimal attack results (approaching TMI) that can be achieved by the average attack prompt composed of each token**.

Case Study. Figure 4 presents a comparative visualization of the routing distribution between RepetitionCurse samples and a balanced baseline on Mixtral-8x7B (Top- $k = 2$). The balanced baseline consists of prompts randomly sampled from LongBench (Bai et al., 2024), truncated to a sequence length of 20,000 tokens to match the RepetitionCurse inputs. It demonstrates that while the MoE router maintains a relatively uniform distribution on natural text, RepetitionCurse inherently induces extreme load concentration.

Assuming we use EP = 2 and experts are assigned to GPUs by index order, such concentration doesn't always translate to optimal latency overhead. For layers where the two highly activated experts are placed on different GPUs (e.g., Layer 1), the load remains evenly split across devices, and no effective delay is incurred despite concentrated routing. However, if we use EP = 8, the theoretically maximum bottleneck can be reached.

3.4. MoE Models Investigation & Setup

To assess the universality of this vulnerability, we scrape 139 MoE models from Huggingface with over 1,000 downloads. We analyze their configuration files to extract the expert and routing strategies. Table 1 summarizes the percentage of different MoE architectures and their average downloads. Notably, over 50% of the surveyed models are Mixtral-like

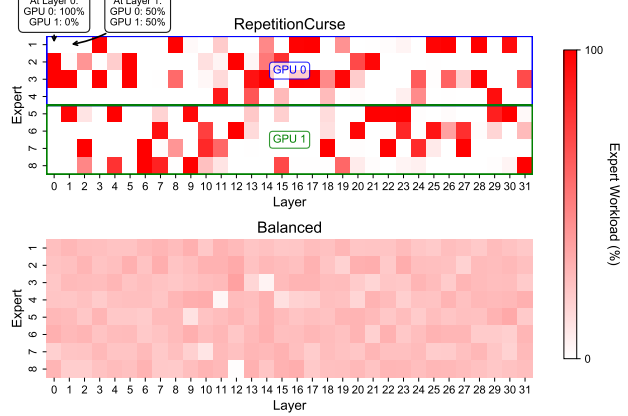


Figure 4. Expert workload comparison between RepetitionCurse and balanced baseline. Each cell represents the expert workload: percentage of tokens routed to the expert.

models, which are characterized by a smaller total number of experts (i.e., 8-16). The remaining models with architectures like DeepSeekV3 and Qwen3Moe are characterized by sparser Top- k experts, with typically only 2 to 12 experts activated from 128 or more experts per token.

Table 1. Summary of surveyed MoE models on Huggingface with their architectures and average downloads.

Pct.	Arch. (Downloads)	Pct.	Arch. (Downloads)
54.68%	Mixtral (9,834)	1.44%	Arctic (4,988)
13.67%	DeepseekV3 (139,431)	1.44%	Deepseek (9,336)
5.76%	Qwen3Moe (325,997)	1.44%	Qwen3Next (885,050)
5.76%	DeepseekV2 (88,858)	1.44%	FlexOlmo (21,874)
2.88%	Olmoe (23,958)	1.44%	Qwen2Moe (27,285)
1.44%	Lfm2Moe (8,346)	1.44%	KimiLinear (157,719)
1.44%	Glm4Moe (4,832)	Others	Jamba, Llama4, Mini-Max, GPT-OSS, ...

Motivated by the investigation, we focus on 14 popular MoE models from the two categories in the experiments, including 4 Mixtral-like low-sparse models and other 10 high-sparse models. Table 2 summarizes their expert configurations and routing strategies. The selected models collectively cover both base and post-trained variants, different attention mechanisms (conventional and linear), and a wide range of expert cardinalities from 8 to 512, enabling a systematic analysis of routing robustness across training stages, architectural choices, and sparsity levels.

4. Experiments

4.1. Coverage Metric

As defined in Section 3.3, Figure 5 presents the bottleneck coverage \mathcal{B} of different models under different EP size. The results are conducted by simulating inference-time behavior using router outputs, under the fact that the assigned

Table 2. Model architectures and attack-related configurations.

Model	L	E	Top- k	$ \mathcal{V} $
Mixtral-8x7B	32	8	2	32000
Mixtral-8x7B-Instruct	32	8	2	32000
Mixtral-8x7B-Chinese	32	8	2	57000
Mixtral-8x7B-Nous	32	8	2	32002
Qwen3-30B-A3B	48	128	8	151936
Qwen3-30B-A3B-Instruct	48	128	8	151936
Qwen3-Coder-30B-A3B-Instruct	48	128	8	151936
Qwen3-Next-30B-A3B	48	512	10	151936
Qwen3-Next-30B-A3B-Thinking	48	512	10	151936
GPT-OSS-20B	24	32	4	201088
GPT-OSS-120B	36	128	4	201088
Kimi-Linear-Instruct	27	256	8	163840
DeepSeek-V2-Lite	27	64	6	102400
Llama-4-Scout-17B-16E-Instruct	48	16	1	202048

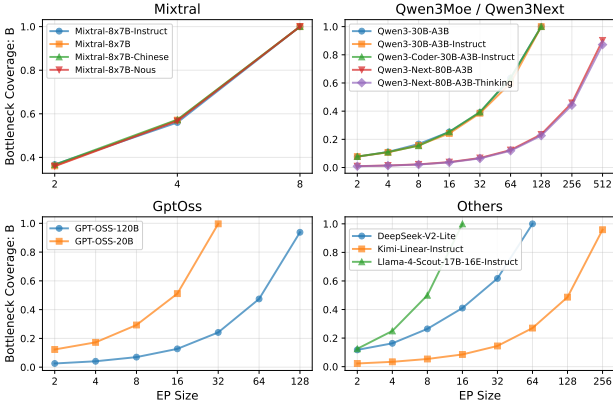


Figure 5. Coverage of different models under different EP size.

tokens number serves as a proxy for its latency. This allows us to evaluate bottleneck coverage under arbitrary expert-GPU mapping without requiring full system execution. We summarize our observations and suggestions as follows:

1. Models from the same family exhibit similar coverage values (e.g., Mixtral-8x7B and its fine-tuned variants). This suggests that **the vulnerability is primarily introduced during pretraining rather than during post-training or instruction tuning**.
2. Bottleneck coverage consistently increases with the EP size, indicating that larger EP configurations exacerbate the vulnerability during the prefill phase. This creates a deployment dilemma: **increasing EP to improve locality and efficiency simultaneously amplifies the attack surface**.
3. When $EP = E$, coverage approaches 1 for all models. This implies that nearly any token in the vocabulary can be used to construct an effective attack prompt, demon-

strating the broad exploitability of the vulnerability. It also highlights that **Mixtral-like models are particularly susceptible to this class of attacks**.

4. Under commonly used EP settings (e.g., 16–64), models with a larger number of experts exhibit lower coverage. Consequently, **more highly sparse models, such as Qwen3Next, show stronger resistance to this attack compared to low-sparsity designs**.

4.2. Latency Metrics

We now evaluate inference latency on MoE models deployed with vLLM under expert parallelism. The process time of each layer can be decomposed to attention part and MoE part. From our investigation of the 14 experimental models, the MoE part typically takes $> 60\%$ of the total layer time. Given the same token number, the attention time is stable due to its dense nature, while the MoE time can be affected by the router results. We examine the impact of RepetitionCurse attack on inference Latency Amplification Ratio (LAR) through two hierarchical metrics.

(1) System-Level LAR. We deploy the target models locally using vLLM with instrumented profiling. We measure the actual execution time of the MoE kernel. Let T_{moe}^i denote the MoE processing time of the i -th layer on the bottleneck GPU, we report R_{moe} as defined in Equation (5).

$$R_{\text{moe}} = \frac{T_{\text{moe}}^i(P_{\text{attack}})}{T_{\text{moe}}^i(P_{\text{normal}})} \quad (5)$$

For each target model, we construct 200 RepetitionCurse prompts and 200 normal prompts, each with a length of 20,000. We test each target model under $EP = 2, 4$ and 8 .

The results are shown in Table 3. As expected, the LAR increases with the increase of EP size. For Mixtral models, the deployment on 8 GPUs resulting in a delay exceeding 150%; for other sparser models, due to the inability of RepetitionCurse to control whether the attacked experts are on the same GPU, the delay under $EP = 8$ is only 31% to 96%. Nevertheless, the trend suggests better attack effects under larger EP size configurations.

(2) End-to-End API LAR. From the perspective of a black-box attacker, we measure the total round-trip time for API requests to indicate the actual performance degradation caused by RepetitionCurse. We define API LAR as:

$$R_{\text{api}} = \frac{T(P_{\text{attack}})}{T(P_{\text{normal}})} \quad (6)$$

For each API, we construct 100 adversarial prompts and 100 normal prompts, each with a length of 20,000. Considering potential network fluctuations, we calculate the point estimate of R_{api} . All adversarial prompts are different to avoid the impact of caching mechanisms. We set

Table 3. The system-level LAR (R_{moe}) of different models under different deployment configurations.

Model	R_{moe}		
	EP ²	EP ⁴	EP ⁸
Mixtral-8x7B	1.492	1.823	2.651
Mixtral-8x7B-Instruct	1.359	1.905	2.534
Mixtral-8x7B-Chinese	1.307	1.962	2.856
Mixtral-8x7B-Nous	1.306	1.885	2.529
Qwen3-30B-A3B	1.197	1.278	1.488
Qwen3-30B-A3B-Instruct	1.238	1.238	1.330
Qwen3-Coder-30B-A3B-Instruct	1.092	1.217	1.310
Qwen3-Next-30B-A3B	1.185	1.323	1.328
Qwen3-Next-30B-A3B-Thinking	1.146	1.258	1.416
GPT-OSS-20B	1.038	1.126	1.247
GPT-OSS-120B	1.009	1.132	1.353
Kimi-Linear-Instruct	1.034	1.047	1.074
DeepSeek-V2-Lite	1.136	1.392	1.429
Llama-4-Scout-17B-16E-Instruct	1.592	1.920	1.968

max_new_tokens to 1 to get TTFT for prefilling performance. The results are shown in Table 4, where we report the average API TTFT of RepetitionCurse and normal prompts, and the 95% confidence lower bound of R_{api} .

The results demonstrate that inference requests constructed using RepetitionCurse consistently incur higher average API TTFT than normal prompts, effectively resulting in a DoS effect. Across the majority of evaluated APIs, the observed LAR exceeds 100%, ranging from $1.514\times$ to $4.728\times$. These findings indicate that RepetitionCurse enables substantially more efficient participation in DoS attacks against online LLM inference services.

4.3. Side-channel Effect

Owing to the structural properties of MoE models, inference latency under RepetitionCurse exhibits distinctive amplification patterns that can serve as a side-channel for inferring backend model architectures and deployment characteristics. Routing-induced imbalance manifests as measurable latency amplification that is absent in dense models.

In Table 4, we first evaluate the APIs of two known dense models, Llama-3-8B-Instruct and Qwen3-14B. In both cases, the measured R_{api} remains close to or less than 1 under RepetitionCurse prompts. In contrast, for all evaluated APIs corresponding to known MoE models, R_{api} consistently exceeds 1 under the same attack.

Furthermore, by comparing R_{api} with locally fitted R_{moe} curves (Table 3), it becomes possible to infer coarse-grained deployment properties, such as the approximate number of GPUs used for expert parallelism. For example, we ob-

Table 4. Comparison of average TTFT between RepetitionCurse and normal prompts, sorted in descending order by R_{api} .

Model	$T(P)$ (s)		R_{api}
	attack	normal	
Dense Models			
Llama-3-8B-Instruct	2.452	1.952	1.160
Qwen3-14B	6.603	7.359	0.635
MoE Models			
Kimi-Linear-Instruct	14.595	2.066	4.728
DeepSeek-R1-Turbo	10.762	1.942	4.012
Qwen3-Coder-30B-A3B-Instruct	17.067	3.454	3.233
Mixtral-8x7B	25.789	5.288	3.063
DeepSeek-Chat	8.435	2.422	2.439
GPT-OSS-20B	6.197	1.672	2.399
GPT-OSS-120B	13.220	2.951	2.341
Qwen3-Next-80B-A3B	7.365	1.952	2.192
Qwen3-30B-A3B	8.080	2.569	2.138
Qwen3-Next-80B-A3B-Thinking	7.678	2.377	2.129
Llama-4-Scout-17B-16E	3.866	2.002	1.514
Undisclosed Architecture			
ChatGPT-3.5-Turbo	8.704	1.850	2.971
ChatGPT-4	4.475	1.702	2.003
ChatGPT-4o-Mini	13.415	3.482	1.772

serve that the R_{api} for models like Kimi-Linear-Instruct and GPT-OSS exceed R_{moe} derived under an 8-GPU configuration, suggesting that the corresponding service backends are likely deployed on larger EP size.

To validate the practicality of this side-channel, we probe the APIs of three ChatGPT models with undisclosed backend architectures. In all cases, we observe $R_{\text{api}} > 1$ significantly (From $1.772\times$) under RepetitionCurse attack, suggesting that these services are likely backed by MoE-based inference systems.

5. Extended Analysis and Implications

5.1. Length Scalability

An important robustness question for the vulnerability exploited by RepetitionCurse is its sensitivity to prompt length: whether inducing routing imbalance necessitates long sequences, or whether similar effects arise under shorter contexts. We investigate this question through experiments on two representative MoE models, Mixtral-8x7B and Qwen3-30B-A3B, spanning prompt lengths ranging from 100 to 16k tokens and five different system prompts.

To characterize expert load concentration from a routing-centric perspective instead of any specific deployment configuration, we measure the normalized entropy $\mathcal{H}(P)$ of the expert selection distribution, averaged across all layers. This metric captures the intrinsic routing behavior induced

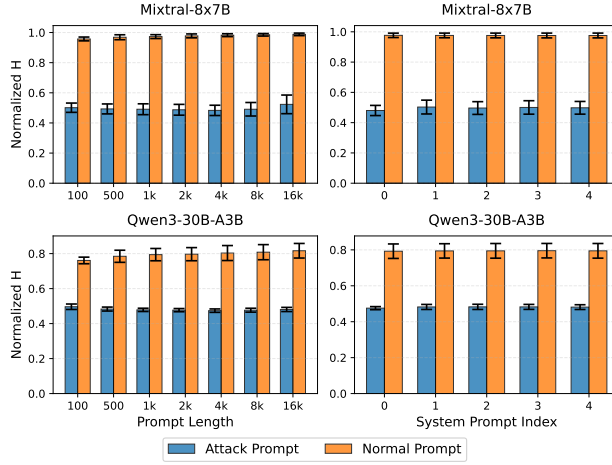


Figure 6. Normalized entropy of the expert selection distribution under different prompt lengths and system prompts.

by a prompt, without relying on device-level bottleneck assumptions. Formally, the normalized entropy is defined as

$$\mathcal{H}(P) = \frac{1}{L} \sum_{l=1}^L \frac{-\sum_{e \in \mathcal{E}_l} \rho_{l,e}(P) \log \rho_{l,e}(P)}{\log E} \quad (7)$$

Lower entropy values correspond to more concentrated expert selection, indicating stronger routing imbalance.

The results shown in Figure 6 demonstrate that RepetitionCurse exhibits length scalability and robustness. We observe that the induced token concentration remains highly consistent across the entire range of tested sequence lengths (100 to 16k tokens). Furthermore, this behavior proves to be invariant to the diversity of system prompts.

This consistency indicates that the vulnerability revealed by RepetitionCurse is systemic in nature of MoE architectures. It suggests that when tokens exhibit repetitive patterns during the prefill phase, their corresponding embeddings are immediately dominated by this repetition. Consequently, the router is manipulated into deterministically assigning these tokens to a fixed set of experts.

5.2. Vulnerable Experts Distribution

We further investigate whether specific experts exhibit inherent vulnerabilities to RepetitionCurse attack. To quantify this, we perform a vocabulary-wide scan for each expert across the target models. Specifically, we count the number of unique tokens in the vocabulary that, when used to construct a RepetitionCurse prompt, result in a routing imbalance exceeding a threshold of $\tau = 90\%$ for that specific expert. This metric identifies vulnerable experts that act as attractors for a disproportionate amount of repetitive tokens.

Figure 7 presents the resulting heatmaps for four models: Mixtral-8x7B, Qwen3-30B-A3B, GPT-OSS-20B, and Kimi-

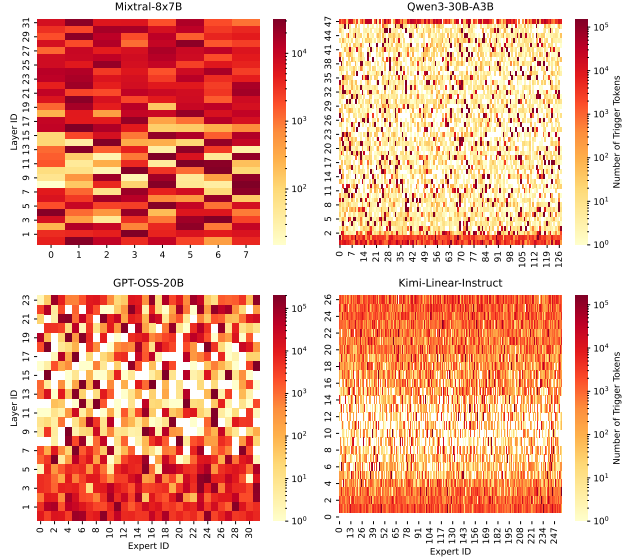


Figure 7. Vulnerable experts distribution. Each cell represents the vulnerable degree of the corresponding expert (v_e).

Linear-Instruct. We observe a compelling and consistent pattern across these models: **experts in the early and late layers generally exhibit broad vulnerability**, where trigger tokens are distributed relatively evenly. In contrast, **the intermediate layers show significant sparsity**, where vulnerability is confined in only a sparse subset of experts.

This distribution feature is most extreme in Qwen3-30B-A3B (Figure 7, top-right). All experts in the first three layers and the final layer accept a comparable magnitude of trigger tokens. However, in the remaining intermediate layers, the vast majority of trigger tokens are routed to a very small number of specific experts (\sim top- k). We hypothesize that this behavior constitutes a fallback mechanism emergent from the training process. These few intermediate experts appear to be designated to handle anomalous or out-of-distribution patterns that don't map to any semantic concept.

5.3. Defense Proposals

Given that RepetitionCurse exposes a generic vulnerability across current MoE architectures capable of significantly degrading inference service availability, we propose two potential defense mechanisms to mitigate this threat.

Anomaly Detection via Perplexity Filtering. A distinguishing feature of RepetitionCurse prompts is their highly repetitive pattern. Unlike optimization-based adversarial prompts such as GCG (Zou et al., 2023), these inputs exhibit extremely low perplexity (PPL). Empirically, for sequences of 20,000 tokens' length, normal prompts converge to a PPL ~ 5 , whereas RepetitionCurse prompts yield PPL ~ 1 .

This gap suggests a potential defense based on PPL thresh-

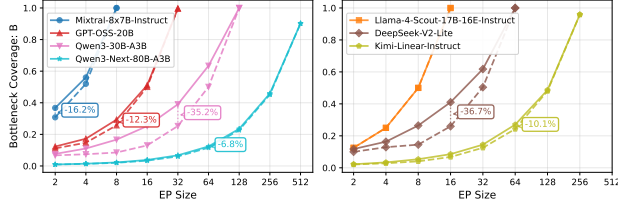


Figure 8. Effect of vulnerability-aware load balance strategy. Solid lines show the bottleneck coverage under the default expert–GPU assignment, while dashed lines correspond to coverage after applying the proposed strategy.

olding; however, introducing an additional PPL evaluation stage requires an auxiliary screening model, incurring extra latency and deployment overhead. Notably, across all evaluated commercial APIs, none of the RepetitionCurse prompts are rejected, indicating that PPL-based filtering is not currently adopted by existing online inference services.

Vulnerability-Aware Load Balance. For highly sparse MoE models, our analysis in Section 5.2 reveals that RepetitionCurse tokens tend to be routed to a small subset of vulnerable experts. This observation motivates a deployment-time defense that explicitly places these vulnerable experts on distinct devices. Under such a placement, even if an adversarial prompt successfully activates all vulnerable experts simultaneously, the resulting computation is distributed across the cluster, preventing the bottleneck and effectively mitigating latency amplification.

To evaluate the effectiveness of this strategy, we simulate EP deployments using a greedy load-balancing algorithm (See Algorithm 1) that assigns experts to GPUs with their vulnerable degrees (defined in Section 5.2). Figure 8 shows the resulting bottleneck coverage \mathcal{B} after rebalancing. We observe that this defense is particularly effective for configurations with a moderate E (e.g., 64–128) and large enough k , where vulnerable experts can be separated across devices. For example, for DeepSeek-V2-Lite ($E = 64, k = 6$), its coverage decreased by 36.7% at EP = 16.

6. Related Work

MoE models and expert parallel. MoE architecture scales model capacity while maintaining low inference costs (Shazeer et al., 2017). Following the success of GPT-4 (OpenAI et al., 2023) and Mixtral (Jiang et al., 2024), MoE has become a standard for LLMs. To support these models, popular inference engines like vLLM (Kwon et al., 2023) and SGLang (Zheng et al., 2024) utilize expert parallelism (EP). Unlike early implementations that risked OOM errors or token dropping during buffer overflows (Hayes et al., 2024), they handle routing congestion by serializing computations rather than crashing, trading latency for memory safety. This risk is further exacerbated by recent trends to

Algorithm 1 Vulnerability-Aware Load Balance

Require: Expert vulnerability degrees $\{v_e\}_{e \in \mathcal{E}_l}$ at layer l , set of devices \mathcal{D}

Ensure: Expert-GPUs mapping $\mathcal{M}_l : \mathcal{D} \rightarrow 2^{\mathcal{E}_l}$

- 1: Initialize per-device vulnerability $V_d \leftarrow 0$ and expert count $C_d \leftarrow 0$ for all $d \in \mathcal{D}$
- 2: Set expert capacity per device $E_d \leftarrow |\mathcal{E}_l|/|\mathcal{D}|$
- 3: Sort experts $e \in \mathcal{E}_l$ in descending order of v_e
- 4: **for** each expert e in sorted order **do**
- 5: Select $d^* = \arg \min_{d \in \mathcal{D}} V_d$ such that $C_d < E_d$
- 6: Assign e to device d^* : $\mathcal{M}_l(d^*) \leftarrow \mathcal{M}_l(d^*) \cup \{e\}$
- 7: Update $V_{d^*} \leftarrow V_{d^*} + v_e, C_{d^*} \leftarrow C_{d^*} + 1$
- 8: **end for**
- 9: **return** \mathcal{M}_l

wards fine-grained experts (e.g., DeepSeek-V3 (DeepSeek-AI et al., 2024b)), where high-degree EP amplifies the synchronization overhead caused by straggler devices.

LLM system-level attacks. LLMs deployed as inference systems have system attack vectors. Hayes et al. (2024) indicates that MoE LLMs using the expert-selects-token mechanism can be vulnerable to buffer overflow attacks, thereby reducing performance on normal tasks. Wu et al. (2025) has studied issues that may lead to privacy leaks in multi-tenant LLM systems with shared KV cache. Gao et al. (2024); Zhang et al. (2025); Li et al. (2025b) explore aspects of launching DoS attacks against LLM systems, including inducing LLM into endless loop outputs, injecting malicious code on systems that allow tool calls to cause resource exhaustion and inducing LLM to think infinitely.

7. Conclusion

In this paper, we uncover a fragile routing imbalance as an inherent attack surface in MoE EP deployment. We show that RepetitionCurse can exploit this vulnerability using simple repetitive token patterns, transforming EP’s efficiency advantage into a severe latency bottleneck and enabling algorithmic DoS attacks. As commercial services increasingly adopt highly sparse MoE models, our results underscore the urgent need for inference-aware routing balance strategies.

Ethical Statement

This paper studies a security vulnerability in MoE inference systems that can be exploited for DoS effects, with the goal of improving the robustness of modern LLM deployments. Experiments on commercial LLM APIs were conducted responsibly, using a limited number of requests within documented rate limits, and DoS effects were assessed via latency rather than direct service disruption.

References

Agrawal, A., Kedia, N., Panwar, A., Mohan, J., Kwatra, N., Gulavani, B. S., Tumanov, A., and Ramjee, R. Tampering throughput-latency tradeoff in LLM inference with sarathi-serve. In Gavrilovska, A. and Terry, D. B. (eds.), *18th USENIX Symposium on Operating Systems Design and Implementation, OSDI 2024, Santa Clara, CA, USA, July 10-12, 2024*, pp. 117–134. USENIX Association, 2024.

Amdahl, G. M. Validity of the single processor approach to achieving large scale computing capabilities. In *Proceedings of the April 18-20, 1967, spring joint computer conference*, pp. 483–485, 1967.

Bai, Y., Tu, S., Zhang, J., Peng, H., Wang, X., Lv, X., Cao, S., Xu, J., Hou, L., et al. Longbench v2: Towards deeper understanding and reasoning on realistic long-context multitasks. *ArXiv preprint arXiv:2412.15204*, 2024.

Cai, W., Jiang, J., Wang, F., Tang, J., Kim, S., and Huang, J. A survey on mixture of experts in large language models. *IEEE Trans. Knowl. Data Eng.*, 37(7):3896–3915, 2025. doi: 10.1109/TKDE.2025.3554028.

DeepSeek-AI. Eplb: Expert parallelism load balancer. <https://github.com/deepseek-ai/EPLB>, 2025. Accessed: 2025-12-14.

DeepSeek-AI, Liu, A., Feng, B., Wang, B., Wang, B., Liu, B., Zhao, C., Dengr, C., Ruan, C., et al. Deepseek-v2: A strong, economical, and efficient mixture-of-experts language model. *arXiv preprint arXiv: 2405.04434*, 2024a.

DeepSeek-AI, Liu, A., Feng, B., Xue, B., Wang, B., Wu, B., Lu, C., Zhao, C., Deng, C., et al. Deepseek-v3 technical report. *arXiv preprint arXiv: 2412.19437*, 2024b.

Du, N., Huang, Y., Dai, A. M., Tong, S., Lepikhin, D., Xu, Y., Krikun, M., Zhou, Y., Yu, A. W., et al. Glam: Efficient scaling of language models with mixture-of-experts. In Chaudhuri, K., Jegelka, S., Song, L., Szepesvári, C., Niu, G., and Sabato, S. (eds.), *International Conference on Machine Learning, ICML 2022, 17-23 July 2022, Baltimore, Maryland, USA*, volume 162 of *Proceedings of Machine Learning Research*, pp. 5547–5569. PMLR, 2022.

Fedus, W., Zoph, B., and Shazeer, N. Switch transformers: Scaling to trillion parameter models with simple and efficient sparsity. *arXiv preprint arXiv: 2101.03961*, 2021.

Gao, K., Pang, T., Du, C., Yang, Y., Xia, S.-T., and Lin, M. Denial-of-service poisoning attacks against large language models. *arXiv preprint arXiv: 2410.10760*, 2024.

Gong, R., Bai, S., Wu, S., Fan, Y., Wang, Z., Li, X., Yang, H., and Liu, X. Past-future scheduler for llm serving under sla guarantees. In *Proceedings of the 30th ACM International Conference on Architectural Support for Programming Languages and Operating Systems, Volume 2*, pp. 798–813, 2025.

Hayes, J., Shumailov, I., and Yona, I. Buffer overflow in mixture of experts. In *Neurips Safe Generative AI Workshop 2024*, 2024.

Jiang, A. Q., Sablayrolles, A., Roux, A., Mensch, A., Savary, B., Bamford, C., Chaplot, D. S., de las Casas, D., Hanna, E. B., et al. Mixtral of experts. *arXiv preprint arXiv: 2401.04088*, 2024.

Kwon, W., Li, Z., Zhuang, S., Sheng, Y., Zheng, L., Yu, C. H., Gonzalez, J. E., Zhang, H., and Stoica, I. Efficient memory management for large language model serving with pagedattention. In *Proceedings of the ACM SIGOPS 29th Symposium on Operating Systems Principles*, 2023.

Li, J., Gao, Y., Yang, Y., Bai, Y., Zhou, X., Li, Y., Sun, H., Liu, Y., Si, X., et al. Fundamental capabilities and applications of large language models: A survey. *ACM Comput. Surv.*, 58(2), 2025a. ISSN 0360-0300. doi: 10.1145/3735632.

Li, Y., Wang, J., Zhu, H., Lin, J., Chang, S., and Guo, M. Thinktrap: Denial-of-service attacks against black-box llm services via infinite thinking. *arXiv preprint arXiv: 2512.07086*, 2025b.

Mu, S. and Lin, S. A comprehensive survey of mixture-of-experts: Algorithms, theory, and applications. *arXiv preprint arXiv: 2503.07137*, 2025.

OpenAI, Achiam, J., Adler, S., Agarwal, S., Ahmad, L., Akkaya, I., Aleman, F. L., Almeida, D., Altenschmidt, J., et al. Gpt-4 technical report. *arXiv preprint arXiv: 2303.08774*, 2023.

Shazeer, N., Mirhoseini, A., Maziarz, K., Davis, A., Le, Q. V., Hinton, G. E., and Dean, J. Outrageously large neural networks: The sparsely-gated mixture-of-experts layer. In *5th International Conference on Learning Representations, ICLR 2017, Toulon, France, April 24-26, 2017, Conference Track Proceedings*. OpenReview.net, 2017.

Shoeybi, M., Patwary, M., Puri, R., LeGresley, P., Casper, J., and Catanzaro, B. Megatron-lm: Training multi-billion parameter language models using model parallelism. *arXiv preprint arXiv: 1909.08053*, 2019.

Sun, Y., Li, Z., Zhang, Y., Pan, T., Dong, B., Guo, Y., and Wang, J. Efficient attention mechanisms for large language models: A survey. *arXiv preprint arXiv: 2507.19595*, 2025.

Vaswani, A., Shazeer, N., Parmar, N., Uszkoreit, J., Jones, L., Gomez, A. N., Kaiser, L., and Polosukhin, I. Attention is all you need. In Guyon, I., von Luxburg, U., Bengio, S., Wallach, H. M., Fergus, R., Vishwanathan, S. V. N., and Garnett, R. (eds.), *Advances in Neural Information Processing Systems 30: Annual Conference on Neural Information Processing Systems 2017, December 4-9, 2017, Long Beach, CA, USA*, pp. 5998–6008, 2017.

vLLM Contributors. Fused MoE modular kernel. https://docs.vllm.ai/en/latest/design/fused_moe_modular_kernel/, 2025.

Wu, G., Zhang, Z., Zhang, Y., Wang, W., Niu, J., Wu, Y., and Zhang, Y. I know what you asked: Prompt leakage via kv-cache sharing in multi-tenant llm serving. In *Proceedings of the 2025 Network and Distributed System Security (NDSS) Symposium. San Diego, CA, USA*, 2025.

Zhang, Y., Wang, W., Zhou, Z., Wang, K., Zhang, J., Sun, L., Liu, Y., and Su, S. Leechhijack: Covert computational resource exploitation in intelligent agent systems. *arXiv preprint arXiv: 2512.02321*, 2025.

Zheng, L., Yin, L., Xie, Z., Sun, C., Huang, J., Yu, C. H., Cao, S., Kozyrakis, C., Stoica, I., et al. Sglang: Efficient execution of structured language model programs. In Globersons, A., Mackey, L., Belgrave, D., Fan, A., Paquet, U., Tomeczak, J. M., and Zhang, C. (eds.), *Advances in Neural Information Processing Systems 38: Annual Conference on Neural Information Processing Systems 2024, NeurIPS 2024, Vancouver, BC, Canada, December 10 - 15, 2024*, 2024.

Zou, A., Wang, Z., Carlini, N., Nasr, M., Kolter, J. Z., and Fredrikson, M. Universal and transferable adversarial attacks on aligned language models. *arXiv preprint arXiv: 2307.15043*, 2023.